

Variational quantum circuit learning of entanglement purification in multi-degree-of-freedom

Hao Zhang,¹ Xusheng Xu,^{2,*} Chen Zhang,^{1,†} Man-Hong Yung,³ Tao Huang,^{1,4,‡} and Yunjie Liu^{1,4}

¹*Purple Mountain Laboratories, Nanjing 211111, China*

²*Department of Physics, State Key Laboratory of Low-Dimensional Quantum Physics, Tsinghua University, Beijing 100084, China*

³*Shenzhen Institute for Quantum Science and Engineering,*

Southern University of Science and Technology, Shenzhen 518055, China

⁴*State Key Laboratory of Networking and Switching Technology,
Beijing University of Posts and Telecommunications, Beijing 100876, China*

(Dated: September 20, 2022)

Quantum entanglement purification (EP) is a crucial technique for promising the effective function of entanglement channel in noisy large-scale quantum network. The previous EP protocols lack of a general circuit framework and become complicated to design in high-dimensional cases. In this paper, we propose a variational quantum circuit framework and demonstrate its feasibility of learning optimal protocols of EP in multi-degree-of-freedom (DoF). By innovatively introducing the additional circuit lines for representing the ancillary DoFs, e.g. space and time, the parameterized quantum circuit can effectively simulate the scalable EP process. As examples, well-known protocols in linear optics including PSBZ, HHSZ+ and etc., are learnt successfully with high fidelities and the alternative equivalent operations are discovered in low-depth quantum circuit. Our work pays the way for exploring the EP protocols with multi-DoF by quantum machine learning.

I. INTRODUCTION

Quantum entanglement which shows the nonlocal correlation between two or more objects is an intriguing phenomenon in quantum mechanics and has no classical counterpart [1]. One usually uses quantum entanglement as a crucial resource for building quantum channel in quantum network [2–6]. However, in practice, entanglement is so fragile in noisy environment that it is hard to be used directly as the effective quantum channel. The reason is that under the influence of noises, the pure maximally entangled state becomes a mixed one. To overcome this problem, a technique called entanglement purification (EP) is proposed to improve the fidelity of damaged entangled state [7–27]. The first EP protocol utilizes another copy of mixed entangled states in Werner form as an auxiliary “target” state and executes the bilateral controlled-NOT (CNOT) operations and parity check to acquire the information of “source” pair [7]. Subsequently, the protocol is developed without requirement of Werner form and has higher efficiency in recursive procedure [8]. The above protocols are based on CNOT gates between two entangled pairs. It is hard to accomplish this operation in experiment especially for photons. Therefore, in optical system, the feasible way is to bring in the ancillary photonic degree-of-freedom (DoF), such as space and time. The first photonic EP protocol which makes use of ancillary DoF is based on selecting the path of entangled pairs [10] and subsequently performed in experiment [19]. Besides, one can design the EP protocol with only one pair of photons with multi-DoF hyperentanglement [11–16, 23–26], e.g. Simon-Pan [11] and HHSZ+ [23] protocols. Up to now, many interesting EP protocols have been proposed for various cases but lack of a general circuit framework. As

the number of entangled pairs and DoFs increase, the optimal design of EP becomes more complicated and challenging.

Fortunately, the numerical simulation provides another effective way to explore the optimal solutions. In recent years, machine learning has been considered for processing quantum information [28–31]. The basic protocols in quantum communication, such as quantum teleportation [32], EP and quantum repeaters [33], are discovered by classical agents [34]. The core model for quantum information processing is quantum gate operations. Therefore, compared with classical machine learning, an approach directly optimizing the quantum gates called variational quantum circuit (VQC) has its inherent advantage for handling quantum information tasks [35–37]. EP, as a key element for quantum network, has been performed as a simple instance in local operation and classical communication (LOCC) framework based on parameterized quantum circuits [38]. However, directly simulating operations on two pairs is limited in some cases, such as difficult CNOT operation of photons. Therefore, the VQC framework for EP including multi-DoF is more general and practical.

In this paper, we propose a VQC framework and demonstrate its feasibility of learning optimal EP with multi-DoF. The additional quantum circuit lines are introduced in VQC to represent the high-dimensional DoFs of particle. In our VQC framework, the encoder circuits can simulate the process of entanglement generation and the decoherence of quantum channel, and the parameterized ansatz part plays the core role in learning the local operations of EP. The classical communications used for exchanging the information between two users are shown in measurement part. As examples, the well-known linear optical EP protocols, including PSBZ [10], HHSZ+ [23], Simon-Pan [11] and etc., are learnt by our VQC learning. Moreover, the different EP operations in linear optics are also discovered easily. Our framework provides the alternative way to understand and design the EP in multi-DoF by quantum machine learning and has extensive applications for other areas of quantum information, such as quantum network.

* thuxxs@163.com

† zhangchen@pmlabs.com.cn

‡ htiao@bupt.edu.cn

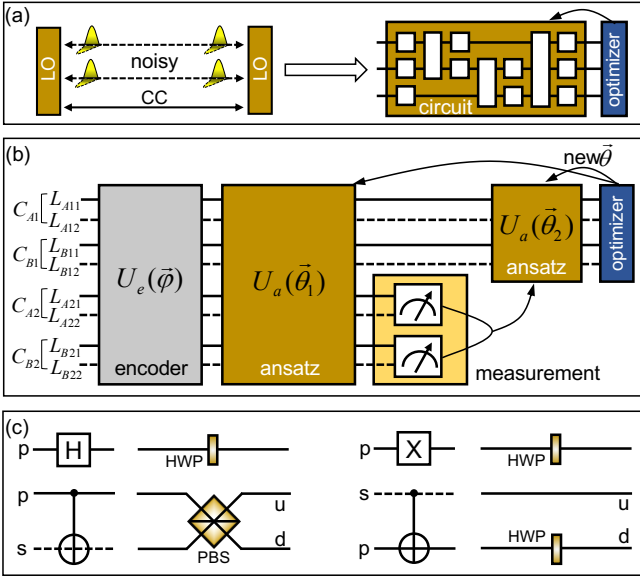


FIG. 1. VQC learning framework of EP with multi-DoF. (a) Simple schematic diagrams of EP in optical system and VQC. LO, local operations; CC, classical communications. (b) An instance for VQC of EP based on polarization and spatial DoFs. (c) The physical implementations of some basic quantum gates in linear optics. The meanings of symbols are: p (s), polarization (spatial) DoF; u (d), up (down) spatial DoF; H, Hadamard gate; X, swap gate; HWP, half-wave plate; PBS, polarizing beam splitter.

The article is organized as follows: In Sec. II, we introduce the VQC learning framework for EP in multi-DoF. In Sec. III, the well-known EP protocols with multi-DoF are learnt. Sec. IV covers discussion and summary.

II. VQC FRAMEWORK FOR EP IN MULTI-DOF

The pure entangled state labelled with ρ_{pure} will become a mixed one ρ_{mixed} when it is distributed over noisy quantum channel. However, the EP is an inverse process which can improve the fidelity of the mixed state. Those two processes can be described by following formula

$$\rho_{\text{pure}} \xrightarrow{\text{noise}} \rho_{\text{mixed}} \xrightarrow{\text{EP}} \rho_{\text{purified}}. \quad (1)$$

Here, ρ_{purified} is density matrix of the purified mixed state and can equal to ρ_{pure} after the perfect EP protocol. In long distance quantum channel, the entangled state is usually shared by two nonlocal quantum nodes shown in left part of Fig. 1 (a). Because of non-locality, two users are only allowed to execute the EP process using LOCC. The local operations are a series of local quantum gates, and the classical communications are used for exchanging the measurement results in two nodes. The VQC shown in right part of Fig. 1 (a) is a hybrid quantum-classical simulator using classical optimizer to optimize parameterized quantum circuits. Here, we propose a specialized VQC framework shown in Fig. 1 (b) to simulate EP. Its architecture also includes quantum encoder, ansatz,

measurement and classical optimizer. The ansatz in this VQC framework has two parts arranged before and after the measurement. The encoder can simulate the entanglement generation and distribution via noisy channels by adding arranged gate operations and noise operators, respectively. If the EP has known initial mixed states, one can omit the encoder and start the process with ansatz directly. The ansatz is the main concern in learning EP and prepared with parameterized quantum circuits based on practical conditions. The gate operations in ansatz between circuit lines of Alice and Bob are forbidden because of only allowing LOCC. The classical communications is shown with curve connecting two measurements. By optimizing the parameterized quantum circuits in ansatz, the process of local operations in EP can be simulated effectively. Each circuit line represents a DoF of entangled particle. We assume that Alice and Bob share n pairs of entangled photons denoted by sets $A = \{A_1, A_2, \dots, A_n\}$ and $B = \{B_1, B_2, \dots, B_n\}$, respectively. A_i and B_i are entangled pair. The photons with m DoFs in sets A and B are also described as sets $A_i = \{D_{Ai1}, D_{Ai2}, \dots, D_{Aim}\}$ and $B_i = \{D_{Bi1}, D_{Bi2}, \dots, D_{Bim}\}$, and the elements D_{Aij} and D_{Bij} stand for different DoFs of photons, such as polarization, space and time. Preparing the quantum circuits in VQC for EP, the circuit lines arranged for Alice and Bob's photons are represented with sets $C_A = \{C_{A1}, C_{A2}, \dots, C_{An}\}$ and $C_B = \{C_{B1}, C_{B2}, \dots, C_{Bn}\}$ respectively. All the elements in sets C_{Ai} and C_{Bi} contain the circuit lines for DoFs of photons and expressed by $C_{Ai} = \{L_{Ai1}, L_{Ai2}, \dots, L_{Aim}\}$ and $C_{Bi} = \{L_{Bi1}, L_{Bi2}, \dots, L_{Bim}\}$. The construction of circuit lines in VQC is actually a map from the entangled photons to lines, i.e. $f: D_{Aij}(D_{Bij}) \mapsto L_{Aij}(L_{Bij})$. The dimension of each line L_{Aij} , L_{Bij} is decided by D_{Aij} , D_{Bij} and has relation of $\dim(L_{Aij}) = \dim(D_{Aij})$, $\dim(L_{Bij}) = \dim(D_{Bij})$. An instance of photons in which two entangled pairs with two DoFs shared by Alice and Bob is given in Fig. 1 (b), the horizontal solid and dashed lines represent the photonic polarization and spatial DoFs, respectively. Circuit lines $C_{A1} = \{L_{A11}, L_{A12}\}$, $C_{A2} = \{L_{A21}, L_{A22}\}$ belong to Alice and $C_{B1} = \{L_{B11}, L_{B12}\}$, $C_{B2} = \{L_{B21}, L_{B22}\}$ are Bob's. Lines C_{A1} , C_{B1} are nonlocal entangled pair, and C_{A2} , C_{B2} are another one. The polarization has horizontal (H) and vertical (V) directions, and spatial DoF is assumed with only up and down. Therefore, the dimension of DoFs is $\dim(L_{Aij}) = \dim(L_{Bij}) = 2$. In EP, the goal is to obtain the output state with higher fidelity, therefore, the learning cost function can be chosen with $f_{\text{out}} = \langle \psi_{\text{target}} | \rho_{\text{out}} | \psi_{\text{target}} \rangle$. Here, the ρ_{out} is density operator of residual entangled pairs after EP, i.e. depending on $U(\vec{\theta})\rho_{\text{in}}U^\dagger(\vec{\theta})$ and measurement. $|\psi_{\text{target}}\rangle$ is the target state. Therefore, when the measurement is chosen, the goal is to train the parameters $\vec{\theta}$. The Fig. 1 (c) shows instances of the physical implementations of several basic quantum gates on polarization and spatial DoFs in linear optics. The half-wave plate (HWP) can act as Hadamard or swap gate of photonic polarization DoF with different input angles. The polarizing beam splitter (PBS) which reflects V and transmits H polarization of photon realizes a CNOT gate on photonic polarization (source) and spatial (target) DoFs. A reversed CNOT between polarization (target) and spatial (source) DoFs can be realized by adding a HWP functioning swap gate in down path.

III. LEARNING ENTANGLEMENT PURIFICATION IN LINEAR OPTICS

A. PSBZ protocol

The four Bell states are usually considered in EP as follows

$$\begin{aligned} |\Phi^\pm\rangle &= \frac{1}{\sqrt{2}}(|00\rangle \pm |11\rangle), \\ |\Psi^\pm\rangle &= \frac{1}{\sqrt{2}}(|01\rangle \pm |10\rangle). \end{aligned} \quad (2)$$

To show the learning function of our VQC framework, we first study the PSBZ EP protocol proposed by Pan et al. [10] for linear optics. In the protocol, the photonic spatial DoF is introduced to overcoming the problem of difficult CNOT operation between photons. The ideal case is that Alice and Bob share Bell pairs $|\Phi_{ab}^\pm\rangle = \frac{1}{\sqrt{2}}(|0_a 0_b\rangle \pm |1_a 1_b\rangle)$ in polarization DoFs from ideal source. Here, the state 0 and 1 in $|\Phi_{ab}^\pm\rangle$ represent for V and H polarization of photon, respectively. The photons labelled with “a” and “b” belong to Alice and Bob, respectively. The mixed state considered with only bit-flip error before EP is given by

$$\rho_{in}^{ab} = f_{in} |\Phi_{ab}^+\rangle \langle \Phi_{ab}^+| + (1 - f_{in}) |\Psi_{ab}^+\rangle \langle \Psi_{ab}^+|. \quad (3)$$

Therefore, the two-copy of this mixed state $\rho_{in}^{a1b1} \otimes \rho_{in}^{a2b2}$ has four components, including $|\Phi_{a1b1}^+\rangle |\Phi_{a2b2}^+\rangle$ with fidelity f_{in}^2 , $|\Phi_{a1b1}^+\rangle |\Psi_{a2b2}^+\rangle$ with fidelity $f_{in}(1 - f_{in})$, $|\Psi_{a1b1}^+\rangle |\Phi_{a2b2}^+\rangle$ with fidelity $f_{in}(1 - f_{in})$, and $|\Psi_{a1b1}^+\rangle |\Psi_{a2b2}^+\rangle$ with fidelity $(1 - f_{in})^2$. Different with BBPSSW [7] and DEJMPS [8] protocols, PSBZ replaces the CNOT between two photons with the CNOT between two DoFs of each photon. As shown in Fig. 2 (a), two symmetric PBSs are used by both Alice and Bob. The whole process is described with quantum circuit language in Fig. 2 (b). For simplicity of calculation, we label the Alice and Bob’s photons with 1, 3, 5, 7 and 2, 4, 6, 8, respectively. Circuit lines 1 (3) and 2 (4) are entangled photons. All the circuit lines 5, 6, 7 and 8 are spatial DoFs and plotted together. The initial state of spatial DoF is $|0_5 0_6 1_7 1_8\rangle$ and 0 (1) stands for up (down) path. The two PBSs play roles in applying four CNOT gates between polarization and spatial DoFs of each photon. Actually, the CNOT gates on all spatial DoFs produce two pairs of four-DoF entangled state. By choosing the measurement result of all output with photon, the residual four polarization DoFs are entangled as

$$\begin{aligned} \rho_{in}^{cnot} &= f_{in}^2 (|0_1 0_2 0_3 0_4\rangle + |1_1 1_2 1_3 1_4\rangle) \langle \dots| \\ &+ (1 - f_{in})^2 (|0_1 1_2 0_3 1_4\rangle + |1_1 0_2 1_3 0_4\rangle) \langle \dots|, \end{aligned} \quad (4)$$

where the symbol $\langle \dots|$ is the bras of corresponding kets in its left brackets. The detailed derivation process is given in Appendix A. Here, the measurement bases $|+\rangle = \frac{1}{\sqrt{2}}(|0\rangle + |1\rangle)$ and $|-\rangle = \frac{1}{\sqrt{2}}(|0\rangle - |1\rangle)$ are used to measure the target pair. If Alice and Bob get the results $|++\rangle$ or $|--\rangle$, the state of source pair is

$$\rho_{12}^{++} = f_{out}^{++} |\Phi_{12}^+\rangle \langle \Phi_{12}^+| + (1 - f_{out}^{++}) |\Psi_{12}^+\rangle \langle \Psi_{12}^+|, \quad (5)$$

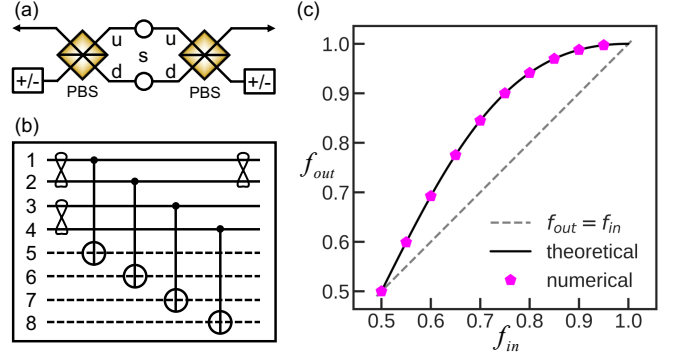


FIG. 2. VQC learning of the PSBZ protocol. (a) The physical schematic diagrams of EP. “s” represents ideal entanglement source. “u” and “d” are up and down spatial DoFs, respectively. (b) The quantum circuit version of PSBZ protocol. (c) Learning and theoretical results of fidelities.

where the new fidelity is $f_{out}^{++} = \frac{f_{in}^2}{f_{in}^2 + (1 - f_{in}^2)}$. When the result is $|+-\rangle$ or $|+ -\rangle$, the output state will be translated to $|\Phi_{12}^+\rangle$, whose new fidelity is $f_{out}^{+-} = f_{out}^{++}$, by applying a local phase flip gate on one of residual photons.

Using VQC framework to learn the above EP protocol, we directly learn the ansatz by assuming a series of parameterized universal quantum gates including single qubit arbitrary rotation gates and two qubit CNOT gates. The input of ansatz is $\rho_{in} = \rho_{a1b1} \otimes \rho_{a2b2} \otimes |0_5 0_6 1_7 1_8\rangle \langle 0_5 0_6 1_7 1_8|$. Our goal is to learn the optimal fidelity of final output state given by cost function $f_{out} = \langle \Phi^+ | \rho_{out} | \Phi^+ \rangle$ (also used in other protocols). The numerical results are shown in Fig. 2 (c). The points in figure are our learning fidelities and match the theoretical curve f_{out}^{++} very well. The learnt ansatz suggests the optimal fidelities of EP as same as PSBZ protocol in Fig. 2 (b) for this input mixed state ρ_{in} . The learnt local operations are not unique due to the learning of fidelity. By assigning the appropriate initial parameters of ansatz, the same local operations in PSBZ are learnt successfully.

B. Hyperentanglement-based protocols

Another kinds of EP protocols using multi-DoF are based on hyperentanglement. Only one pair of photons entangled in both polarization and spatial DoFs are required. The Bell states of polarization and spatial DoFs have same form with Eq. (2) and are labelled with $|\Phi_p^\pm\rangle$, $|\Psi_p^\pm\rangle$, $|\Phi_s^\pm\rangle$ and $|\Psi_s^\pm\rangle$. Subscripts “p” and “s” represent polarization and spatial DoFs, respectively. The typical EP protocols based on hyperentanglement are HHSZ+ [23], Simon-Pan [11], Li [12] and Sheng-Deng [13] and etc.. We first study the HHSZ+ protocol whose initial state is described by $\rho_{in} = \rho_{in}^p \otimes \rho_{in}^s$, where the density operators ρ_{in}^p and ρ_{in}^s are

$$\rho_{in}^p = f_{in}^p |\Phi_p^+\rangle \langle \Phi_p^+| + (1 - f_{in}^p) |\Psi_p^+\rangle \langle \Psi_p^+|, \quad (6)$$

and

$$\rho_{in}^s = f_{in}^s |\Phi_s^+\rangle \langle \Phi_s^+| + (1 - f_{in}^s) |\Psi_s^+\rangle \langle \Psi_s^+|. \quad (7)$$

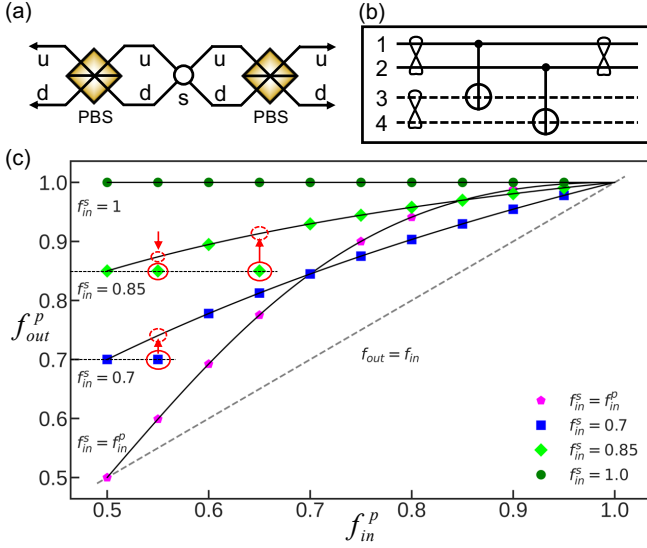


FIG. 3. VQC learning of the HHSZ+ and Simon-Pan protocols with hyperentanglement. (a) The physical schematic diagrams of two protocols. (b) The quantum circuit version of two protocols. Lines 1 (2) and 3 (4) are polarization and spatial DoFs of photon belongs to Alice (Bob), respectively. (c) Learning and theoretical results of fidelities.

Here, f_{in}^p and f_{in}^s are fidelities of $|\Phi_p^+\rangle$ and $|\Phi_s^+\rangle$, respectively. The equivalent EP using time DoF is ESBHBU protocol [24]. Here, only one entangled pair and two PBSs are required for accomplishing EP of polarization DoF shown in Fig. 3 (a) when input fidelities satisfy $f_{in}^p > \frac{1}{2}$ and $f_{in}^s > \frac{1}{2}$. In VQC framework, two polarization and another two spatial lines are introduced in Fig. 3 (b). Compared with PSBZ protocol, the physical devices are the same but the quantum circuit only has two CNOT gates in HHSZ+. Shown in Appendix B, the output fidelity is $f_{out}^p = \frac{f_{in}^p f_{in}^s}{f_{in}^p f_{in}^s + (1-f_{in}^p)(1-f_{in}^s)}$ for the selection of $|0_3 0_4\rangle$ (two up) or $|1_3 1_4\rangle$ (two down). Three cases are considered as $f_{in}^p = f_{in}^s$, $f_{in}^p \neq f_{in}^s$ and $f_{in}^s = 1$ in numerical learning. For $f_{in}^p \neq f_{in}^s$, we learn the output fidelities by fixing the f_{in}^s with 0.7 and 0.85. When the fidelity satisfies $f_{in}^s = 1$, the HHSZ+ transforms to Simon-Pan protocol. As shown in Fig. 3 (c), the curve of $f_{out}^p = f_{in}^p$ is the same with PSBZ protocol. It's worth noting that the learning points labelled with red solid ellipses, two points of $f_{in}^s = 0.85$ and one point of $f_{in}^s = 0.7$, below the theoretical curve are not the optimal points and this phenomenon is so called local minimum in numerical simulation which can be corrected by multi-round computing with different initial parameters. The dashed circles with arrows show the optimal points corresponding to those local minimal points. Those local minimal points with value $f_{out}^p = f_{in}^s$ indicates exchanging ρ_{in}^p with ρ_{in}^s will obtain the output entangled pairs with a better fidelity than f_{in}^p . For instance, if the square with red ellipse of $\rho_{in}^p = 0.7$ is executed with HHSZ+ protocol, it will be the dashed circle in the theoretical curve. But the learnt local optimal point suggest a swap operation to exchange the state between polarization and spatial DoFs. This operation will obtain a higher fidelity in polarization DoF, i.e. $f_{out}^p = 0.7 > f_{in}^p = 0.55$, but is not the optimal. In $f_{in}^s = 1$, the

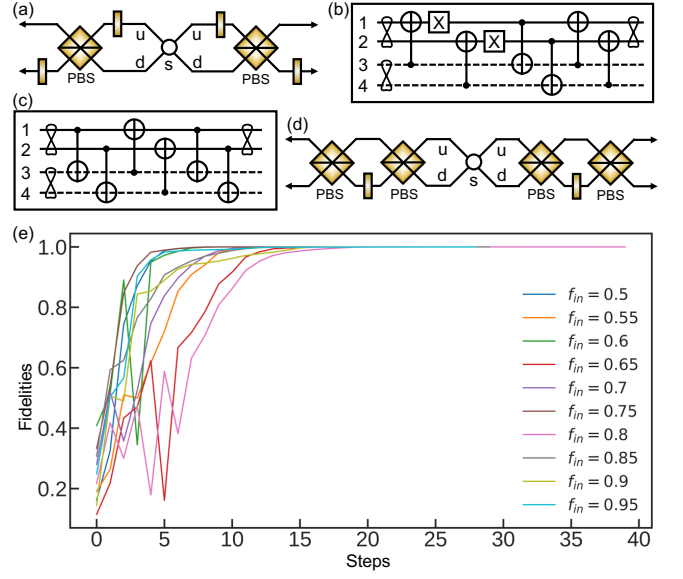


FIG. 4. VQC learning of the Li protocol with hyperentanglement. (a) The physical schematic diagrams of Li protocol. (b) The corresponding quantum circuit of Li protocol. Lines 1 (2) and 3 (4) are polarization and spatial DoFs of photon belongs to Alice (Bob), respectively. (c) The quantum circuit of an example of new equivalent EP protocols learnt by VQC. (d) The physical schematic diagrams of new equivalent EP circuit in (c). (e) Learning curves of chosen fidelities based on VQC with a set of random initial parameters.

output purified state is a pure entangled state and total probability of four cases with spatial output $|0_5 0_6\rangle$, $|0_5 1_6\rangle$, $|1_5 0_6\rangle$ and $|1_5 1_6\rangle$ is 100%. Results in Fig. 3 (c) indicates all the assumed cases are discovered by our VQC framework and the learnt local operations are the same as Fig. 3 (b) with appropriate initial parameters.

If we study the case considering the phase error, the terms $|\Phi^-\rangle\langle\Phi^-|$ and $|\Psi^-\rangle\langle\Psi^-|$ are added in density operators. When the spatial DoF is a pure entangled state, the corresponding EPs are Li [12] and Sheng-Deng [13] protocols. As an instance, we simulate the Li protocol here. The detailed explanations of Li protocol are given in Appendix C. Compared with Simon-Pan, the operations in this case need at least three bilateral CNOT gates in Alice and Bob. The physical implementation and its corresponding quantum circuit of Li protocol are plotted in Fig. 4 (a) and (b). By VQC learning, the Li protocol is also learnt successfully. Moreover, the results of optimized parameters in ansatz also suggest some other different local operations whose final outputs are the same with Li's. We show one of the equivalent protocols discovered by VQC learning in Fig. 4 (c) and (d) with quantum circuit and setup versions where four PBSs and two HWPs are used. The learning curves of fidelities are shown in Fig. 4 (e). With about only 20 steps, all the 10 processes achieve their optimal fidelities. In learning processes of aforementioned typical protocols, the initial parameters of parameterized quantum circuit are assigned randomly, but the learning results show the symmetric operations in Alice and Bob which are consistent with all the theoretical protocols.

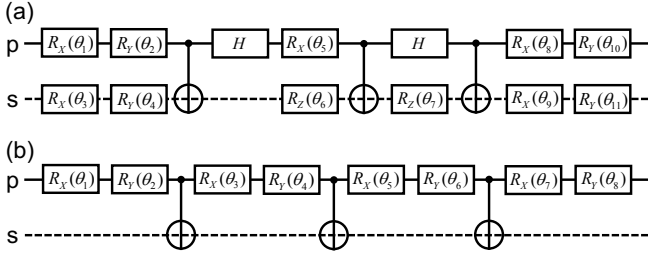


FIG. 5. The quantum circuits of ansatz used in our simulations between two different DoFs. (a) An universal quantum circuit for two-qubit operations. (b) A limited ansatz with no single-qubit operations in spatial DoF. $R_X(\theta_i)$ and $R_Y(\theta_i)$ are gates rotating the state around the X and Y-axis with angle θ_i , respectively.

IV. DISCUSSION AND SUMMARY

The initial circuits of ansatz used in our simulations are given in Fig. 5 (a) and (b). The ansatz with $\vec{\theta}_u = [\theta_1, \theta_2, \dots, \theta_{11}]$ in Fig. 5 (a) is an universal quantum circuit for two-qubit operations with a series of single-qubit operations and three CNOT gates [39]. In some practical cases, the operations can not be done with experimental conditions. Therefore, we introduce a limited ansatz with $\vec{\theta}_l = [\theta_1, \theta_2, \dots, \theta_8]$ by assuming the single qubit operations are difficult in spatial DoF in Fig. 5 (b). In performance of above protocols, we learn the optimal fidelities by universal ansatz and then repeat the process with limited one if we need. The parameters vector $\vec{\theta}_u$ in universal ansatz is assigned with random numbers in domain $[0, 2\pi]$, i.e. the learning curves are usually different in each round, but the final stationary results are almost the same (the local minimum appears with small probability can be eliminated by repeating more times). In simulations, we find that the learnt ansatz is sensitive to the initial value of parameters. If we only use the universal ansatz with random values in $[0, 2\pi]$, the learnt operations are probably different with PSBZ because of non-uniqueness of the global optimum in fidelity-based learning. The closer optimal parameters with respective to initial values are easier to be learnt. In PSBZ protocol, the same operations can be learnt easily when the initial parameters of ansatz is close to theoretical values, i.e. $\vec{\theta}_l$ assigned with small values $[0, 2\pi] * \epsilon$. All the codes for our simulations will be shared in Mindquantum [40].

Besides the learning function for optimal design, our VQC framework provides another perspective for understanding the EP process. For instance, the physical device and the optical path are the same for PSBZ and HHSZ+ protocols, i.e. Fig. 2 (b) and Fig. 3 (b), but the principles are absolutely different. This difference can be viewed clearly in quantum circuit language. PSBZ protocol executes the four CNOT gates between polarization and spatial DoFs, but the HHSZ+ performs two CNOTs. The circuit lines in PSBZ and HHSZ+ protocols are eight and four, respectively.

In conclusion, we propose a VQC framework for learning EP with multi-DoF by introducing the additional circuit lines. To demonstrate the learning function, the well-known protocols of EP in linear optics, such as PSBZ, HHSZ+, Simon-Pan

and etc., are learnt and matched well with theoretical values. Moreover, the alternative operations for EP also can be discovered. Our work not only creates a way to design optimal EP by quantum machine learning, but also gives the new comprehension of EP in quantum circuit language.

Appendix A: PSBZ protocol in quantum circuit language

The density operator of initial mixed state is described as

$$\rho_{12} = \rho_{34} = f_{in} |\Phi_{ab}^+\rangle \langle \Phi_{ab}^+| + (1 - f_{in}) |\Psi_{ab}^+\rangle \langle \Psi_{ab}^+|. \quad (A1)$$

Therefore, the system composed of two entangled pairs has density operator given by

$$\begin{aligned} \rho_{1-4} &= \rho_{12} \otimes \rho_{34} \\ &= [f_{in}^2 |\Phi_{12}^+\rangle \langle \Phi_{12}^+| \otimes |\Phi_{34}^+\rangle \langle \Phi_{34}^+| \\ &\quad + f_{in}(1 - f_{in}) |\Phi_{12}^+\rangle \langle \Phi_{12}^+| \otimes |\Psi_{34}^+\rangle \langle \Psi_{34}^+| \\ &\quad + f_{in}(1 - f_{in}) |\Psi_{12}^+\rangle \langle \Psi_{12}^+| \otimes |\Phi_{34}^+\rangle \langle \Phi_{34}^+| \\ &\quad + (1 - f_{in})^2 |\Psi_{12}^+\rangle \langle \Psi_{12}^+| \otimes |\Psi_{34}^+\rangle \langle \Psi_{34}^+|]. \end{aligned} \quad (A2)$$

The state of spatial DoF at the beginning is a product state expressed with $\rho_{5-8} = |0_5 0_6 1_7 1_8\rangle \langle 0_5 0_6 1_7 1_8|$, where 0 and 1 stand for up and down path, respectively. The density operator of whole system composed of two DoFs can be written as

$$\begin{aligned} \rho_{1-8} &= \rho_{1-4} \otimes \rho_{5-8} \\ &= \frac{1}{4} [f_1 (|0_1 0_2 0_3 0_4 0_5 0_6 1_7 1_8\rangle + |1_1 1_2 0_3 0_4 0_5 0_6 1_7 1_8\rangle) \\ &\quad + |0_1 0_2 1_3 1_4 0_5 0_6 1_7 1_8\rangle + |1_1 1_2 1_3 1_4 0_5 0_6 1_7 1_8\rangle) \langle \dots| \\ &\quad + f_2 (|0_1 0_2 0_3 1_4 0_5 0_6 1_7 1_8\rangle + |1_1 1_2 0_3 1_4 0_5 0_6 1_7 1_8\rangle) \\ &\quad + |0_1 0_2 1_3 0_4 0_5 0_6 1_7 1_8\rangle + |1_1 1_2 1_3 0_4 0_5 0_6 1_7 1_8\rangle) \langle \dots| \\ &\quad + f_2 (|0_1 1_2 0_3 0_4 0_5 0_6 1_7 1_8\rangle + |1_1 0_2 0_3 0_4 0_5 0_6 1_7 1_8\rangle) \\ &\quad + |0_1 1_2 1_3 1_4 0_5 0_6 1_7 1_8\rangle + |1_1 0_2 1_3 1_4 0_5 0_6 1_7 1_8\rangle) \langle \dots| \\ &\quad + f_3 (|0_1 1_2 0_3 1_4 0_5 0_6 1_7 1_8\rangle + |1_1 0_2 0_3 1_4 0_5 0_6 1_7 1_8\rangle) \\ &\quad + |0_1 1_2 1_3 0_4 0_5 0_6 1_7 1_8\rangle + |1_1 0_2 1_3 0_4 0_5 0_6 1_7 1_8\rangle) \langle \dots|]. \end{aligned}$$

Here, the symbol $\langle \dots|$ means they are the bras of corresponding kets in their left brackets. Fidelities f_1 , f_2 and f_3 are $f_1 = f_{in}^2$, $f_2 = f_{in}(1 - f_{in})$ and $f_3 = (1 - f_{in})^2$. The PBS has the function of a CNOT gate whose control qubit is polarization and the target is spatial DoF as follows

$$\begin{aligned} U_{CNOT}^{PBS} &= \bigotimes_{i=1}^4 (|0_i 0_{i+4}\rangle \langle 0_i 0_{i+4}| + |0_i 1_{i+4}\rangle \langle 0_i 1_{i+4}| \\ &\quad + |1_i 1_{i+4}\rangle \langle 1_i 0_{i+4}| + |1_i 0_{i+4}\rangle \langle 1_i 1_{i+4}|). \end{aligned} \quad (A3)$$

Here, the state 0 and 1 represent V and H polarization, respectively. After CNOT gate operations on states of all spatial

DoFs, two entangled pairs become

$$\begin{aligned}\rho_{1-8}^{cnot} &= U_{CNOT}^{PBS} \rho_{1-8} U_{CNOT}^{PBS\dagger} \\ &= \frac{1}{4} [f_1(|0_1 0_2 0_3 0_4 0_5 0_6 1_7 1_8\rangle + |1_1 1_2 0_3 0_4 1_5 1_6 1_7 1_8\rangle \\ &\quad + |0_1 0_2 1_3 1_4 0_5 0_6 0_7 0_8\rangle + |1_1 1_2 1_3 1_4 1_5 1_6 0_7 0_8\rangle) \langle \dots| \\ &\quad + f_2(|0_1 0_2 0_3 1_4 0_5 0_6 1_7 0_8\rangle + |1_1 1_2 0_3 1_4 1_5 1_6 1_7 0_8\rangle \\ &\quad + |0_1 0_2 1_3 0_4 0_5 0_6 0_7 1_8\rangle + |1_1 1_2 1_3 0_4 1_5 1_6 0_7 1_8\rangle) \langle \dots| \\ &\quad + f_2(|0_1 1_2 0_3 0_4 0_5 1_6 1_7 1_8\rangle + |1_1 0_2 0_3 0_4 1_5 0_6 1_7 1_8\rangle \\ &\quad + |0_1 1_2 1_3 1_4 0_5 1_6 0_7 0_8\rangle + |1_1 0_2 1_3 1_4 1_5 0_6 0_7 0_8\rangle) \langle \dots| \\ &\quad + f_3(|0_1 1_2 0_3 1_4 0_5 1_6 1_7 0_8\rangle + |1_1 0_2 0_3 1_4 1_5 0_6 1_7 0_8\rangle \\ &\quad + |0_1 1_2 1_3 0_4 0_5 1_6 0_7 1_8\rangle + |1_1 0_2 1_3 0_4 1_5 0_6 0_7 1_8\rangle) \langle \dots|].\end{aligned}$$

If one chooses the case of all four output ports with one photon, i.e. $|0_5 0_6 1_7 1_8\rangle$, $|1_5 1_6 0_7 0_8\rangle$, $|0_5 1_6 1_7 0_8\rangle$, $|1_5 0_6 0_7 1_8\rangle$, this selection will project the system on spatial state $|\psi_{5678}\rangle = \frac{1}{2}(|0_5 0_6 1_7 1_8\rangle + |1_5 1_6 0_7 0_8\rangle + |0_5 1_6 1_7 0_8\rangle + |1_5 0_6 0_7 1_8\rangle)$. The polarization DoFs are projected into state

$$\begin{aligned}\rho_{1-4}^{cnot} &= \langle \psi_{5678} | \rho_{1-8} | \psi_{5678} \rangle \\ &= \frac{1}{16} [f_{in}^2(|0_1 0_2 0_3 0_4\rangle + |1_1 1_2 1_3 1_4\rangle) \langle \dots| \\ &\quad + (1 - f_{in})^2(|0_1 1_2 0_3 1_4\rangle + |1_1 0_2 1_3 0_4\rangle) \langle \dots|].\end{aligned}\quad (A4)$$

When the measurement results in Alice and Bob are obtained with $|+3 +4\rangle$ or $|-3 -4\rangle$ where $|+\rangle$ and $|-\rangle$ are $|+\rangle = \frac{1}{\sqrt{2}}(|0\rangle + |1\rangle)$ and $|-\rangle = \frac{1}{\sqrt{2}}(|0\rangle - |1\rangle)$ respectively, the state is chosen with

$$\begin{aligned}\rho_{12}^{++} &= \langle +3 +4 | \rho_{1-4}^{cnot} | +3 +4 \rangle \\ &= \langle -3 -4 | \rho_{1-4}^{cnot} | -3 -4 \rangle \\ &= \frac{1}{64} [f_{in}^2 |\Phi_{12}^+\rangle \langle \Phi_{12}^+| + (1 - f_{in})^2 |\Psi_{12}^+\rangle \langle \Psi_{12}^+|].\end{aligned}\quad (A5)$$

If the measurement results are $|+3 -4\rangle$ or $|-3 +4\rangle$, the state got by Alice and Bob is

$$\begin{aligned}\rho_{12}^{+-} &= \langle +3 -4 | \rho_{1-4}^{cnot} | +3 -4 \rangle \\ &= \langle -3 +4 | \rho_{1-4}^{cnot} | -3 +4 \rangle \\ &= \frac{1}{64} [f_{in}^2 |\Phi_{12}^-\rangle \langle \Phi_{12}^-| + (1 - f_{in})^2 |\Psi_{12}^-\rangle \langle \Psi_{12}^-|].\end{aligned}\quad (A6)$$

For this case, Alice or Bob should make a local phase flip gate on her/his photon to obtain the target state $|\Phi_{12}^+\rangle$.

Appendix B: HHSZ+ and Simon-Pan protocols

Considering HHSZ+ protocol [23] in which a hyperentanglement in both polarization and spatial DoFs is used, the state of a system is $\rho_{in} = \rho_p \otimes \rho_s$. Here, ρ_p and ρ_s are the density operators of polarization and spatial DoFs, respectively. The Bell states of spatial DoF are given by

$$\begin{aligned}|\Phi_s^\pm\rangle &= \frac{1}{\sqrt{2}}(|0_3 0_4\rangle \pm |1_3 1_4\rangle), \\ |\Psi_s^\pm\rangle &= \frac{1}{\sqrt{2}}(|0_3 1_4\rangle \pm |1_3 0_4\rangle).\end{aligned}\quad (B1)$$

As shown in Fig. 3 (b), we use subscripts 1 (3) and 2 (4) to label the polarization (spatial) DoFs of Alice and Bob, respectively. The hyperentanglement is distributed to Alice and Bob, and will be a mixed one via a noisy channel given by

$$\rho_{in}^p = f_{in}^p |\Phi_p^+\rangle \langle \Phi_p^+| + (1 - f_{in}^p) |\Psi_p^+\rangle \langle \Psi_p^+|, \quad (B2)$$

and

$$\rho_{in}^s = f_{in}^s |\Phi_s^+\rangle \langle \Phi_s^+| + (1 - f_{in}^s) |\Psi_s^+\rangle \langle \Psi_s^+|. \quad (B3)$$

The coefficients f_{in}^p and f_{in}^s are the initial fidelities of polarization and spatial DoFs, respectively. The fidelities satisfy conditions $f_{in}^p > \frac{1}{2}$ and $f_{in}^s > \frac{1}{2}$. Therefore, the state of whole system is

$$\begin{aligned}\rho_{1-4} &= \rho_{12} \otimes \rho_{34} \\ &= \frac{1}{4} [f_1(|0_1 0_2\rangle + |1_1 1_2\rangle)(|0_3 0_4\rangle + |1_3 1_4\rangle) \langle \dots| \\ &\quad + f_2(|0_1 0_2\rangle + |1_1 1_2\rangle)(|0_3 1_4\rangle + |1_3 0_4\rangle) \langle \dots| \\ &\quad + f_3(|0_1 1_2\rangle + |1_1 0_2\rangle)(|0_3 0_4\rangle + |1_3 1_4\rangle) \langle \dots| \\ &\quad + f_4(|0_1 1_2\rangle + |1_1 0_2\rangle)(|0_3 1_4\rangle + |1_3 0_4\rangle) \langle \dots|],\end{aligned}$$

where fidelities f_1, f_2, f_3 and f_4 are $f_1 = f_{in}^p f_{in}^s$, $f_2 = f_{in}^p (1 - f_{in}^s)$, $f_3 = f_{in}^s (1 - f_{in}^p)$ and $f_4 = (1 - f_{in}^p)(1 - f_{in}^s)$. To purify the above states, the bilateral CNOT gates realized by two PBSs are applied as

$$U_{CNOT}^{PBS} = \bigotimes_{i=1}^2 (|0_i 0_{i+2}\rangle \langle 0_i 0_{i+2}| + |0_i 1_{i+2}\rangle \langle 0_i 1_{i+2}| + |1_i 1_{i+2}\rangle \langle 1_i 0_{i+2}| + |1_i 0_{i+2}\rangle \langle 1_i 1_{i+2}|). \quad (B4)$$

After the CNOT operations, the system is transferred to

$$\begin{aligned}\rho_{1-4}^{cnot} &= U_{CNOT}^{PBS} \rho_{1-4} U_{CNOT}^{PBS\dagger} \\ &= \frac{1}{4} [f_1(|0_1 0_2 0_3 0_4\rangle + |1_1 1_2 1_3 1_4\rangle \\ &\quad + |0_1 0_2 1_3 1_4\rangle + |1_1 1_2 0_3 0_4\rangle) \langle \dots| \\ &\quad + f_2(|0_1 0_2 0_3 1_4\rangle + |1_1 1_2 1_3 0_4\rangle \\ &\quad + |0_1 0_2 1_3 0_4\rangle + |1_1 1_2 0_3 1_4\rangle) \langle \dots| \\ &\quad + f_3(|0_1 1_2 0_3 1_4\rangle + |1_1 0_2 1_3 0_4\rangle \\ &\quad + |0_1 1_2 1_3 0_4\rangle + |1_1 0_2 0_3 1_4\rangle) \langle \dots| \\ &\quad + f_4(|0_1 1_2 0_3 0_4\rangle + |1_1 0_2 1_3 1_4\rangle \\ &\quad + |0_1 1_2 1_3 1_4\rangle + |1_1 0_2 0_3 0_4\rangle) \langle \dots|].\end{aligned}\quad (B5)$$

Analysing above density operator, we find that there are four cases, $0_3 0_4$, $0_3 1_4$, $1_3 0_4$ and $1_3 1_4$, for obtaining the final entangled pair. The case $0_3 0_4$ (two up) and $1_3 1_4$ (two down) induce system with $\rho'_{12} = f_{in}^p f_{in}^s |\Phi_p^+\rangle \langle \Phi_p^+| + (1 - f_{in}^p)(1 - f_{in}^s) |\Psi_p^+\rangle \langle \Psi_p^+|$. So the residual entangled pair $|\Phi_p^+\rangle$ has fidelity $f_{out}^p = \frac{f_{in}^p f_{in}^s}{f_{in}^p f_{in}^s + (1 - f_{in}^p)(1 - f_{in}^s)}$. With conditions $f_{in}^p > \frac{1}{2}$ and $f_{in}^s > \frac{1}{2}$, it has higher fidelity, i.e. $f_{out}^p > f_{in}^p$ and $f_{out}^p > f_{in}^s$.

In some special cases, such as strong robustness of spatial or time DoFs in experiments [25, 26], the entanglement of this robust DoF is nearly pure state, e.g. $f_s = 1$ in Eq. (B3). The

EP of this case is Simon-Pan protocol [11]. In Eq. (B5), if the spatial fidelity is $f_s = 1$, the density operator after CNOTs is

$$\begin{aligned}\rho_{1-4}^{cnot} &= U_{CNOT}^{PBS} \rho_{1-4} U_{CNOT}^{PBS\dagger} \\ &= \frac{1}{4} [f_p(|0_1 0_2 0_3 0_4\rangle + |1_1 1_2 1_3 1_4\rangle \\ &\quad + |0_1 0_2 1_3 1_4\rangle + |1_1 1_2 0_3 0_4\rangle) \langle \dots| \\ &\quad + (1-f_p)(|0_1 1_2 0_3 1_4\rangle + |1_1 0_2 1_3 0_4\rangle \\ &\quad + |0_1 1_2 1_3 0_4\rangle + |1_1 0_2 0_3 1_4\rangle) \langle \dots|].\end{aligned}\quad (B6)$$

One can see that cases $0_3 0_4$ and $1_3 1_4$ with probability f_p will produce $|\Phi_p^+\rangle$, and $0_3 1_4$ and $1_3 0_4$ with probability $1-f_p$ obtain $|\Psi_p^+\rangle$ which can be transformed to $|\Phi_p^+\rangle$ by a local bit-flip operation. The fidelity of purified state is 1.

Appendix C: Li and Sheng-Deng protocols

The EP using hyperentanglement for cases considering the both bit-flip and phase errors of polarization are Li [12] and Sheng-Deng [13] protocols. When considering the phase errors, the density operator will be added with two terms of phase error and becomes

$$\begin{aligned}\rho_{in}^p &= f_{in}^{p1} |\Phi_p^+\rangle \langle \Phi_p^+| + f_{in}^{p2} |\Psi_p^+\rangle \langle \Psi_p^+| \\ &\quad + f_{in}^{p3} |\Phi_p^-\rangle \langle \Phi_p^-| + f_{in}^{p4} |\Psi_p^-\rangle \langle \Psi_p^-|,\end{aligned}\quad (C1)$$

where fidelities satisfy $f_{in}^{p4} = 1 - f_{in}^{p1} - f_{in}^{p2} - f_{in}^{p3}$. And the entangled spatial DoF is ideal $\rho_s = |\Phi_s^+\rangle \langle \Phi_s^+|$. As shown in Fig. 4 (a) and (b), four HWPs used in up and down paths act as CNOT gates whose control and target qubits are spatial and polarization DoFs, respectively. The two kinds of CNOT operations are

$$\begin{aligned}U_{CNOT}^u &= \bigotimes_{i=1}^2 (|1_i 0_{i+2}\rangle \langle 0_i 0_{i+2}| + |0_i 1_{i+2}\rangle \langle 0_i 1_{i+2}| \\ &\quad + |0_i 0_{i+2}\rangle \langle 1_i 0_{i+2}| + |1_i 1_{i+2}\rangle \langle 1_i 1_{i+2}|),\end{aligned}\quad (C2)$$

and

$$\begin{aligned}U_{CNOT}^d &= \bigotimes_{i=1}^2 (|0_i 0_{i+2}\rangle \langle 0_i 0_{i+2}| + |1_i 1_{i+2}\rangle \langle 0_i 1_{i+2}| \\ &\quad + |1_i 0_{i+2}\rangle \langle 1_i 0_{i+2}| + |0_i 1_{i+2}\rangle \langle 1_i 1_{i+2}|).\end{aligned}\quad (C3)$$

Here, U_{CNOT}^u and U_{CNOT}^d are corresponding to HWP in up and down paths, respectively. So, with a series of operations in sequence of bilateral up-CNOT, PBS-CNOT and down-CNOT gates shown in Fig. 4 (a) and (b), the entangled pair is gov-

erned by U_{dpu} as follows

$$\begin{aligned}U_{dpu} &= U_{CNOT}^d U_{CNOT}^{PBS} U_{CNOT}^u \\ &= \bigotimes_{i=1}^2 (|0_i 0_{i+2}\rangle \langle 0_i 0_{i+2}| + |1_i 1_{i+2}\rangle \langle 0_i 1_{i+2}| \\ &\quad + |1_i 0_{i+2}\rangle \langle 1_i 1_{i+2}| + |0_i 1_{i+2}\rangle \langle 0_i 0_{i+2}|).\end{aligned}\quad (C4)$$

The final state of system is calculated as

$$\begin{aligned}\rho &= U_{dpu}(\rho_p \otimes \rho_s) U_{dpu}^\dagger \\ &= f_{in}^{p1} (|0_1 0_2 1_3 1_4\rangle + |0_1 0_2 0_3 0_4\rangle \\ &\quad + |1_1 1_2 1_3 1_4\rangle + |1_1 1_2 0_3 0_4\rangle) \langle \dots| \\ &\quad + f_{in}^{p2} (|0_1 0_2 1_3 0_4\rangle + |0_1 0_2 0_3 1_4\rangle \\ &\quad + |1_1 1_2 1_3 0_4\rangle + |1_1 1_2 0_3 1_4\rangle) \langle \dots| \\ &\quad + f_{in}^{p3} (|0_1 0_2 1_3 1_4\rangle - |0_1 0_2 0_3 0_4\rangle \\ &\quad + |1_1 1_2 1_3 1_4\rangle - |1_1 1_2 0_3 0_4\rangle) \langle \dots| \\ &\quad + f_{in}^{p4} (|0_1 0_2 1_3 0_4\rangle - |0_1 0_2 0_3 1_4\rangle \\ &\quad + |1_1 1_2 1_3 0_4\rangle - |1_1 1_2 0_3 1_4\rangle) \langle \dots|.\end{aligned}\quad (C5)$$

Analysing above density operator, one can find that all the four cases of spatial DoF, i.e. $0_3 0_4$, $0_3 1_4$, $1_3 0_4$ and $1_3 1_4$ will obtain the $|\Phi_p^+\rangle$ with fidelity 1.

The learning results show that all the three gates arranged with the sequences p-s-CNOT (p is control bit and s is target), s-p-CNOT (s is control bit and p is target), p-s-CNOT and s-p-CNOT can realize the same goal with Li protocol. Some kinds of gate combinations are given as follows. The d-p-d gate is

$$\begin{aligned}U_{dpd} &= U_{CNOT}^d U_{CNOT}^{PBS} U_{CNOT}^d \\ &= \bigotimes_{i=1}^2 (|0_i 0_{i+2}\rangle \langle 0_i 0_{i+2}| + |1_i 1_{i+2}\rangle \langle 1_i 1_{i+2}| \\ &\quad + |1_i 0_{i+2}\rangle \langle 0_i 1_{i+2}| + |0_i 1_{i+2}\rangle \langle 1_i 0_{i+2}|).\end{aligned}\quad (C6)$$

The above d-p-d gate equals to p-d-p gate, i.e. $U_{pdp} = U_{CNOT}^{PBS} U_{CNOT}^d U_{CNOT}^{PBS} = U_{dpd}$. The p-d-p gate is shown as an example in Fig. 4 (c) and (d). The u-p-u gates is expressed by

$$\begin{aligned}U_{upu} &= U_{CNOT}^u U_{CNOT}^{PBS} U_{CNOT}^u \\ &= \bigotimes_{i=1}^2 (|1_i 0_{i+2}\rangle \langle 1_i 0_{i+2}| + |0_i 1_{i+2}\rangle \langle 0_i 1_{i+2}| \\ &\quad + |0_i 0_{i+2}\rangle \langle 1_i 1_{i+2}| + |1_i 1_{i+2}\rangle \langle 0_i 0_{i+2}|).\end{aligned}\quad (C7)$$

It is also equal to p-u-p gates as $U_{pup} = U_{CNOT}^{PBS} U_{CNOT}^u U_{CNOT}^{PBS} = U_{upu}$. Another gates u-p-d is written by

$$\begin{aligned}U_{upd} &= U_{CNOT}^u U_{CNOT}^{PBS} U_{CNOT}^d \\ &= \bigotimes_{i=1}^2 (|1_i 0_{i+2}\rangle \langle 0_i 0_{i+2}| + |0_i 1_{i+2}\rangle \langle 1_i 1_{i+2}| \\ &\quad + |0_i 0_{i+2}\rangle \langle 0_i 1_{i+2}| + |1_i 1_{i+2}\rangle \langle 1_i 0_{i+2}|).\end{aligned}\quad (C8)$$

-
- [1] R. Horodecki, P. Horodecki, M. Horodecki, and K. Horodecki, Quantum entanglement, *Rev. Mod. Phys.* **81**, 865 (2009).
 - [2] J. I. Cirac, P. Zoller, H. J. Kimble, and H. Mabuchi, Quantum state transfer and entanglement distribution among distant nodes in a quantum network, *Phys. Rev. Lett.* **78**, 3221 (1997).
 - [3] H. J. Kimble, The quantum internet, *Nature (London)* **453**, 1023 (2008).
 - [4] S. Wehner, D. Elkouss, and R. Hanson, Quantum internet: a vision for the road ahead, *Science* **362**, eaam9288 (2018).
 - [5] H. Zhang, Y. Li, C. Zhang, and T. Huang, Connection-oriented and connectionless quantum internet considering quantum repeaters, *arXiv:2208.03930* (2022).
 - [6] G. L. Long, D. Pan, Y. Sheng, Q. Xue, J. Lu, and L. Hanzo, An evolutionary pathway for the quantum internet relying on secure classical repeaters, *IEEE Network*, **36**, 82-88 (2022).
 - [7] C. H. Bennett, G. Brassard, S. Popescu, B. Schumacher, J. A. Smolin, and W. K. Wootters, Purification of noisy entanglement and faithful teleportation via noisy channels, *Phys. Rev. Lett.* **76**, 722, (1996).
 - [8] D. Deutsch, A. Ekert, R. Jozsa, C. Macchiavello, S. Popescu, and A. Sanpera, Quantum privacy amplification and the security of quantum cryptography, *Phys. Rev. Lett.* **77**, 2818 (1996).
 - [9] C. H. Bennett, D. P. DiVincenzo, J. A. Smolin, and W. K. Wootters, Mixed-state entanglement and quantum error correction, *Phys. Rev. A* **54**, 3824 (1996).
 - [10] J. W. Pan, C. Simon, C. Brukner, and A. Zeilinger, Entanglement purification for quantum communication, *Nature (London)* **410**, 1067 (2001).
 - [11] C. Simon, J. W. Pan, Polarization entanglement purification using spatial entanglement, *Phys. Rev. Lett.* **89**, 257901 (2002).
 - [12] X. H. Li, Deterministic polarization-entanglement purification using spatial entanglement, *Phys. Rev. A* **82**, 044304 (2010).
 - [13] Y. B. Sheng and F. G. Deng, One-step deterministic polarization-entanglement purification using spatial entanglement, *Phys. Rev. A* **82**, 044305 (2010).
 - [14] Y. B. Sheng and F. G. Deng, Deterministic entanglement purification and complete nonlocal Bell-state analysis with hyperentanglement, *Phys. Rev. A* **81**, 032307 (2010).
 - [15] B. C. Ren, F. F. Du, and F. G. Deng, Two-step hyperentanglement purification with the quantum-state-joining method, *Phys. Rev. A* **90**, 052309 (2014).
 - [16] G. Y. Wang, Q. Liu, and F. G. Deng, Hyperentanglement purification for two-photon six-qubit quantum systems, *Physical Review A*, **94**, 032319 (2016).
 - [17] H. Zhang, Q. Liu, X. S. Xu, et al., Polarization entanglement purification of nonlocal microwave photons based on the cross-Kerr effect in circuit QED, *Phys. Rev. A* **96**, 052330 (2017).
 - [18] S. Krastanov, V. V. Albert, and L. Jiang, Optimized entanglement purification, *Quantum* **3**, 123 (2019).
 - [19] J. W. Pan, S. Gasparoni, R. Ursin, G. Weihs, and A. Zeilinger, Experimental entanglement purification of arbitrary unknown states, *Nature (London)* **423**, 417 (2003).
 - [20] R. Reichle, D. Leibfried, E. Knill, et al., Experimental purification of two-atom entanglement, *Nature (London)* **443**, 838 (2006).
 - [21] L. K. Chen, H. L. Yong, P. Xu, et al., Experimental nested purification for a linear optical quantum repeater, *Nat. Photonics* **11**, 695 (2017).
 - [22] N. Kalb, A. A. Reiserer, P. C. Humphreys, et al., Entanglement distillation between solid-state quantum network nodes, *Science* **356**, 928 (2017).
 - [23] X. M. Hu, C. X. Huang, Y. B. Sheng, L. Zhou, et al., Long-distance entanglement purification for quantum communication, *Phys. Rev. Lett.* **126**, 010503 (2021).
 - [24] S. Ecker, P. Sohr, L. Bulla, M. Huber, M. Bohmann, and R. Ursin, Experimental single-copy entanglement distillation, *Phys. Rev. Lett.* **127**, 040506 (2021).
 - [25] C. X. Huang, X. M. Hu, B. H. Liu, L. Zhou, Y. B. Sheng, C. F. Li, and G. C. Guo, Experimental one-step deterministic polarization entanglement purification, *Sci. Bull.* **67**, 593 (2022).
 - [26] S. Ecker, P. Sohr, L. Bulla, R. Ursin, and M. Bohmann, Remotely establishing polarization entanglement over noisy polarization channels, *Phys. Rev. Appl.* **17**, 034009 (2022).
 - [27] H. Yan, Y. Zhong, H. S. Chang, et al., Entanglement purification and protection in a superconducting quantum network, *Phys. Rev. Lett.* **128**, 080504 (2022).
 - [28] J. Biamonte, P. Wittek, N. Pancotti, P. Rebentrost, N. Wiebe, and J. Biamonte, Quantum machine learning, *Nature (London)* **549**, 195 (2017).
 - [29] V. Dunjko and H. J. Briegel, Machine learning & artificial intelligence in the quantum domain: a review of recent progress, *Rep. Prog. Phys.* **81**, 074001 (2018).
 - [30] G. Carleo, I. Cirac, K. Cranmer, L. Daudet, M. Schuld, N. Tishby, L. Vogt-Maranto, and L. Zdeborová, Machine learning and the physical sciences, *Rev. Mod. Phys.* **91**, 045002 (2019).
 - [31] K. Bharti, A. Cervera-Lierta, T. H. Kyaw, et al., Noisy intermediate-scale quantum algorithms, *Rev. Mod. Phys.* **94**, 015004 (2022).
 - [32] C. H. Bennett, G. Brassard, C. Crépeau, et al., Teleporting an unknown quantum state via dual classical and Einstein-Podolsky-Rosen channels, *Phys. Rev. Lett.* **70**, 1895 (1993).
 - [33] H. J. Briegel, W. Dür, J. I. Cirac, and P. Zoller, Quantum repeaters: the role of imperfect local operations in quantum communication, *Phys. Rev. Lett.* **81**, 5932 (1998).
 - [34] J. Wallnöfer, A. A. Melnikov, W. Dür, and H. J. Briegel, Machine learning for long-distance quantum communication, *PRX Quantum* **1**, 010301 (2020).
 - [35] A. Peruzzo, J. McClean, P. Shadbolt, M. Yung, X. Zhou, P. J. Love, A. Aspuru-Guzik, and J. L. O'Brien, A variational eigenvalue solver on a photonic quantum processor, *Nat. Commun.* **5**, 4213 (2014).
 - [36] J. R. McClean, J. Romero, R. Babbush, and A. Aspuru-Guzik, The theory of variational hybrid quantum-classical algorithms, *New J. Phys.* **18**, 023023 (2016).
 - [37] M. Cerezo, A. Arrasmith, R. Babbush, et al., Variational quantum algorithms, *Nat. Rev. Phys.* **3**, 625-644 (2021).
 - [38] X. Zhao, B. Zhao, Z. Wang, Z. Song, and X. Wang, Practical distributed quantum information processing with LOCCNet, *npj Quantum Inf.* **7**, 159 (2021).
 - [39] G. Vidal and C. M. Dawson, Universal quantum circuit for two-qubit transformations with three controlled-NOT gate, *Phys. Rev. A* **69**, 010301 (2004).
 - [40] MindQuantum Developer, MindQuantum: a general software library supporting the development of applications for quantum computation, <https://gitee.com/mindspore/mindquantum>.